



# **iJRASET**

International Journal For Research in  
Applied Science and Engineering Technology



---

# **INTERNATIONAL JOURNAL FOR RESEARCH**

IN APPLIED SCIENCE & ENGINEERING TECHNOLOGY

---

**Volume: 4    Issue: VI    Month of publication: June 2016**

**DOI:**

**[www.ijraset.com](http://www.ijraset.com)**

**Call:  08813907089**

**E-mail ID: [ijraset@gmail.com](mailto:ijraset@gmail.com)**

# Influence of Aluminum Doping on the Magnetic Properties of Li-Zn Spinel Ferrite

G.C. Wakde<sup>1</sup>, A.S. Kakde<sup>2</sup>, P.S. Gaikar<sup>3</sup>, C.M. Dudhe<sup>4</sup>, P.R. Arjunwadkar<sup>5</sup>

<sup>1</sup>Department of Physics, Narayanrao Kale Smruti Model College, Karanja, Wardha 442203, India

<sup>2</sup>Department of Physics, Dr. Ambedkar College, Diksha Bhoomi, Nagpur 440001, India

<sup>3,4,5</sup>Department of Physics, Government Institute of Science, R. T. Road, Nagpur 440001, India

**Abstract-** Lithium ferrite or doped-lithium ferrite are sustainable and potential magnetic material for the microwave applications. A series of Lithium-Zinc spinel ferrites doped by aluminium having general chemical formula  $\text{Li}_{0.5(1-x)}\text{Zn}_x\text{Fe}_{2.5-y}\text{Al}_{y-0.5x}\text{O}_4$  with  $x=0.1$  and  $y = 0.2, 0.4, 0.6$  and  $0.8$  have been synthesized by using precursor citrate sol-gel combustion method. The samples have been subjected to detailed study of magnetic properties. The hysteresis loop of the investigated spinel ferrite sample shows soft ferromagnetic nature. The magnetic parameters such as saturation magnetization, coercivity, remanent magnetization, anisotropy constant, squareness and Bohr Magneton number determined by vibrating sample magnetometer (VSM) measurement. The Curie temperature of the samples decreases with increase in  $\text{Al}^{3+}$  concentration.

**Key Words-** Scanning electron microscopy (SEM), Vibrating sample magnetometer (VSM), Hysteresis curve parameter, Curie temperature.

## I. INTRODUCTION

Recent developments in materials science have stimulated a lot of research interest on lithium and substituted lithium ferrite as it promises to be a potential magnetic material for microwave applications such as; circulators, phase shifters, isolators, power transformation in electronics, memory core, antennas and high-speed digital tapes [1]. Lithium ferrite is an exceptional replacement for microwave applications in place of garnet because of its advantageous characteristics like high saturation magnetization, square hysteresis loop, relatively high Curie temperature and low-cost [2]. Also the lithium ferrite is one of the most versatile magnetic materials for multilayer chip inductor (MLCI) applications and surface mount devices (SMD) due to their high electrical resistivity, low sintering temperature and high permeability [3].

There are several reports on the effect of magnetic and non-magnetic substitutions on various properties of lithium ferrite [4-6]. The magnetic properties of lithium ferrite can be tailored by suitable doping of metal cations and controlling the synthesis process for microwave applications. In the present communication, it is aimed to study the influence of  $\text{Al}^{3+}$  doping on the magnetic parameters of Li-Zn (LZA) spinel ferrite. The variations in Curie temperature, saturation magnetization, coercivity, remanent magnetization, anisotropy constant and Bohr magneton number are studied by using the vibrating sample magnetometer and Gouy's balance characterization technique.

## II. EXPERIMENTAL

Lithium nitrate ( $\text{LiNO}_3$ ,  $\geq 99.0\%$ , Sigma-Aldrich), Zinc nitrate hexa hydrated ( $\text{Zn}(\text{NO}_3)_2 \cdot 6\text{H}_2\text{O}$ ,  $\geq 98.0\%$ , Sigma-Aldrich), Aluminum nitrate nona hydrated ( $\text{Al}(\text{NO}_3)_3 \cdot 9\text{H}_2\text{O}$ ,  $\geq 98.5\%$ , Merck), Iron (III) nitrate nona hydrated ( $\text{Fe}(\text{NO}_3)_3 \cdot 9\text{H}_2\text{O}$ ,  $\geq 99.0\%$ , Merck), Citric acid mono hydrated ( $\text{C}_6\text{H}_8\text{O}_7 \cdot \text{H}_2\text{O}$ ,  $\geq 99.5\%$ , Merck), Ammonia solution ( $\text{NH}_3$ , 25%, Merck) and deionized water were used as raw material for the synthesis of Aluminium substituted Lithium-Zinc ferrite.

A series of aluminium substituted Lithium-Zinc (LZA) spinel ferrite having general formula  $\text{Li}_{0.5(1-x)}\text{Zn}_x\text{Fe}_{2.5-y}\text{Al}_{y-0.5x}\text{O}_4$  (with  $x=0.1$  and  $y = 0.2, 0.4, 0.6$  and  $0.8$ ) have been prepared through citrate sol-gel combustion. Metal nitrate were dissolved together in a minimum amount of deionized water with continuous stirring till clear solution obtained. The citric acid solution was mixed with metal nitrate solution in 1:1 stoichiometric molar ratio. The pH 7 was maintained by adding slowly drop wise ammonia solution into the mixture. The solution was moved on to hot plate with continuous stirring at  $80^\circ\text{C}$  to convert sol into desired gel which was combusted at  $500^\circ\text{C}$  to form a fluffy ash powder. The as-burnt powder sintered at  $800^\circ\text{C}$  for 4 hr. The synthesized samples for  $y = 0.2, 0.4, 0.6, 0.8$  are represented as S1C1, S1C2, S1C3 and S1C4 respectively.

The magnetic parameters are measured by using Lakeshore VSM 7410 vibrating sample magnetometer (VSM) at room temperature.

## International Journal for Research in Applied Science & Engineering Technology (IJRASET)

The susceptibility and curie temperature of the reported sample were determined by using Gouy's balance method.

### III. RESULTS AND DISCUSSION

The hysteresis loops of all the samples of the series LZA spinel ferrite measured at room temperature show that the magnetization first increases rapidly with increasing field up to 4000 G and then increases slowly and saturates at nearly 8000 G of applied magnetic field as shown in the fig 1. The thin hysteresis loop of the entire investigated ferrite sample shows soft ferromagnetic nature with low coercivity [7]. The magnetic parameters such as saturation magnetization, coercivity, remanent magnetization, anisotropy constant, squareness and Bohr Magneton number determined by vibrating sample magnetometer (VSM) measurements of all samples of the series LZA spinel ferrite are presented in the table I.

**TABLE I**

Sample Code	Conc. y	D (nm)	$M_s$ (emu/g)	$H_c$ (G)	$M_r$ (emu/g)	S	K	$n_B$
S1C1	0.2	21.14	54.71	50.063	3.524	0.06441	2853.07	2.0183
S1C2	0.4	20.48	45.76	67.055	3.65	0.07976	3196.29	1.6410
S1C3	0.6	19.76	34.15	90.713	3.808	0.11151	3226.93	1.1894
S1C4	0.8	20.99	21.43	111.36	4.023	0.18773	2485.88	0.7243

GRAIN SIZE, SATURATION MAGNETIZATION ( $M_s$ ), COERCIVE FIELD ( $H_c$ ), REMANENT MAGNETIZATION ( $M_r$ ), SQUARENESS (S), MAGNETIC ANISOTROPY CONSTANT (K) AND BOHR MAGNETON NUMBER of all SAMPLES of SERIES LZA at ROOM TEMPERATURE

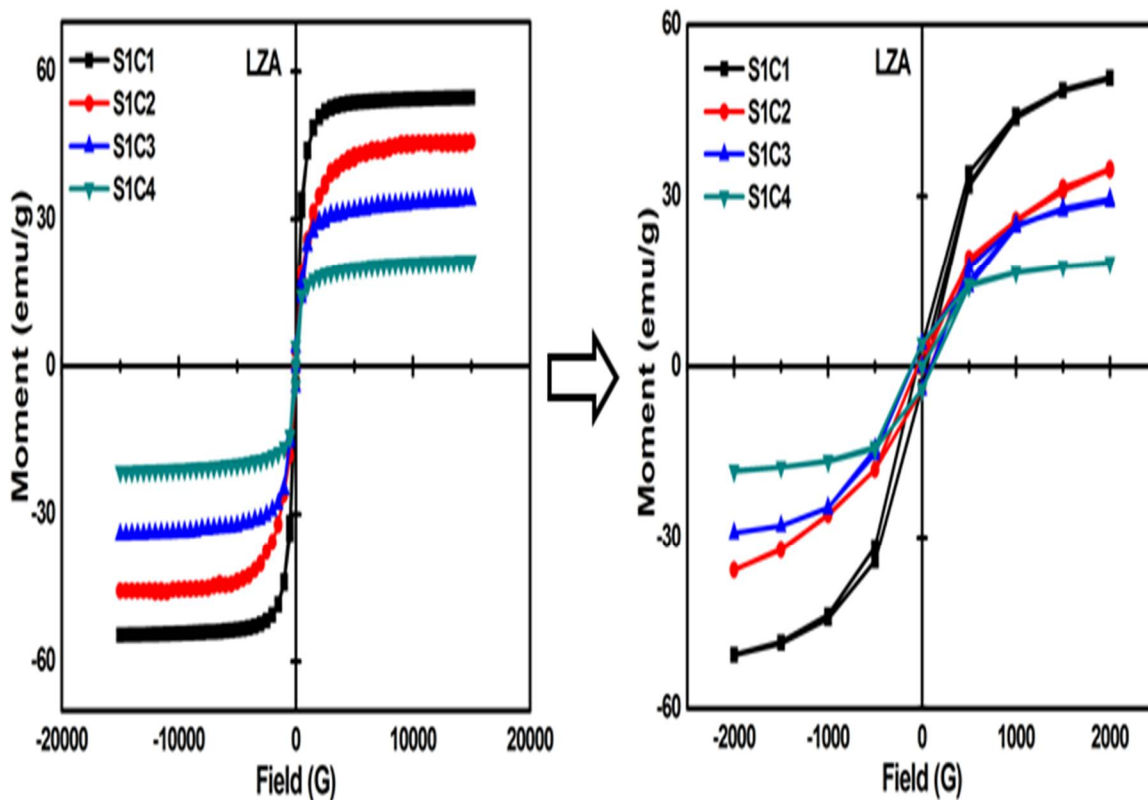


Fig. 1: Hysteresis loop of all samples of the series LZA spinel ferrite at room temperature

## International Journal for Research in Applied Science & Engineering Technology (IJRASET)

The saturation magnetization ( $M_S$ ) has been observed to be decrease with increase in  $Al^{3+}$  concentration for series LZA spinel ferrite as shown in the fig. 2(a). The variation of the saturation magnetization can be explained on the basis of Neel's two sublattice models [8]. According to Neel, there are three kinds of exchange interactions between unpaired electrons of the ions i.e. A-A interaction, B-B interaction and A-B interaction. Among of these, the A-B super-exchange interaction is the predominant interaction over intra-sublattice B-B and A-A interactions. These interactions tend to align all the magnetic spins at A-site in one direction and those at B-site in the opposite direction. Thus the net magnetic moment of the lattice is the vector sum of the magnetic moments of the individual A and B sublattices, given by the following relation:

$$M_S = M_B - M_A \quad \text{---- (1)}$$

Where  $M_S$  is the saturation magnetization,  $M_B$  and  $M_A$  are the magnetization of B and A sublattice respectively. Thus  $M_S$  decreases with substitution of non-magnetic  $Al^{3+}$  ions in place of  $Fe^{3+}$  at octahedral B- sublattice which results in overall reduction of magnetization at B-sublattice and weakens the magnetic A-B exchange interaction [9-10]. The saturation magnetization ( $M_S$ ) values of the nanoparticle in the present investigation are found to be in the range 54.71 emu/g to 21.43 emu/g for LZA spinel ferrite have lower saturation magnetization than that of bulk Li-ferrite ( $\approx 65$  emu/g). However, the non-collinearity if any in the spin arrangement between two sublattices may also contribute in reducing the saturation magnetization. Similar kinds of magnetic hysteresis behaviors have been found in nanosized Li-ferrite prepared by auto-combustion methods [11-12].

The values of coercivity steadily increases from 50 G to 111 G for series LZA spinel ferrite with increase in  $Al^{3+}$  concentration as shown in fig. 2(b). Coercivity of ferrites depends on various parameters like magneto crystalline anisotropy, lattice imperfections, dislocations, internal strains, particle size and secondary phases [13-14]. The variation of the coercivity is mainly influenced by the grain size. It is well known that the coercivity is inversely proportional to grain size [15]. The observed variation of the coercivity and grain size as a function of concentration for series LZA spinel ferrites are presented in the fig. 2(b) which is completely in agreement with the discussion made above.

The value of remanent magnetization ( $M_r$ ) is increases from 3.524 emu /g to 4.023 emu/ g with the substitution of  $Al^{3+}$  ions for LZA spinel ferrite. The compositional variation of remanent magnetization ( $M_r$ ) is shown in the fig. 2(c). The squareness ratio (SQR) is essentially a measure of ratio of remanent magnetization ( $M_r$ ) and saturation magnetization ( $M_s$ ) of the hysteresis loop represented as:

$$S = \frac{M_r}{M_s} \quad \text{---- (2)}$$

If the squareness ration takes the value of about 0.5, it implies that the sample is produces of single magnetic domains [16]. It also determines whether the intergrain exchange exists i.e. for randomly oriented non-interacting particles  $S = 0.5$ , while for  $S < 0.5$  the particles interact by magnetostatic interactions and for  $S > 0.5$  the exchange coupled interaction exists [17-18]. Since, the squareness ratio values range from 0.06 to 0.19 for series LZA which are typical of single domain magnetic grains composed in the structure and the particles interact by magnetostatic interactions as the  $S < 0.5$ . The Bohr magneton numbers, i.e. the saturation magnetization per formula unit in Bohr magnetons ( $n_B$ ) are calculated by using the following relation [19]:

$$n_B = \frac{M_w \times M_s}{5585} \quad \text{---- (3)}$$

Where,  $M_w$  is the molecular weight of composition (in grams),  $M_s$  is the saturation magnetization and 5585 is the magnetic factor. It has been observed from the fig. 2(d) that the magneton number is gradually decreases with increase in  $Al^{3+}$  content of the series LZA spinel ferrite. The value of the anisotropy constant is calculated by using the following relation:

$$H_c = \frac{0.96 \times K}{M_s} \quad \text{---- (4)}$$

The value of anisotropy constant varies from 2853 – 2485 for series LZA spinel ferrite. It is observed that the values of anisotropy constant decreases with the increases in  $Al^{3+}$  concentration for all samples of the series LZA spinel ferrite.

## International Journal for Research in Applied Science & Engineering Technology (IJRASET)

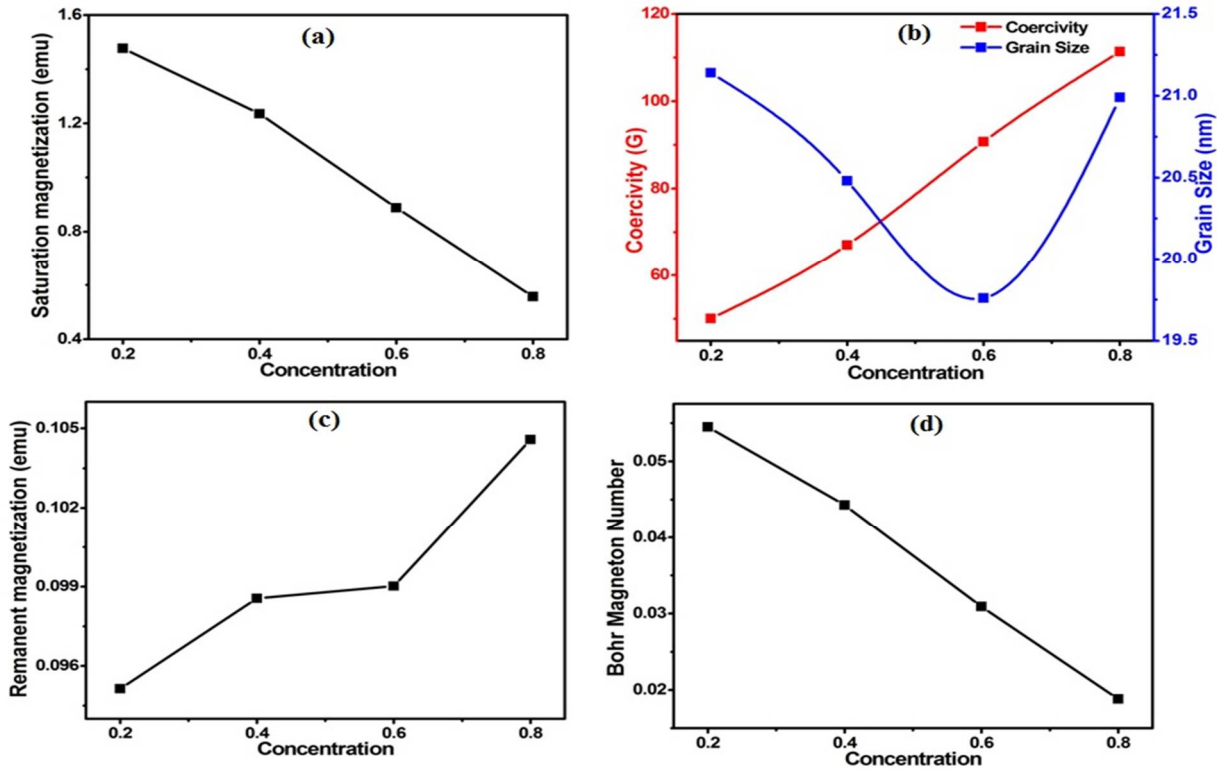


Fig. 2: (a) Compositional variation of saturation magnetization (b) Compositional variation of coercivity and grain size (c) Compositional variation of remanent magnetization (d) Compositional variation of Bohr magneton number of all samples of the series LZA spinel ferrite.

The plot of the inverse of magnetic susceptibility ( $1/\chi$ ) versus temperature (K) of all samples of the series LZA spinel ferrite is presented in the fig. 3(a). It can be observed from the fig. 3 that the values of inverse of magnetic susceptibility ( $1/\chi$ ) increases with enhancement in temperature in the ferrimagnetic region followed by a sudden increase at the certain temperature due to the loss of magnetization representing transition to the paramagnetic region. The temperature at which a magnetically ordered material becomes magnetically disordered, i.e. becomes paramagnet is known as the Curie temperature ( $T_C$ ). The values of Curie temperature ( $T_C$ ) are calculated by extrapolating the paramagnetic region to the X-axis. The values of the Curie temperature for series LZA spinel ferrite are listed in the table II.

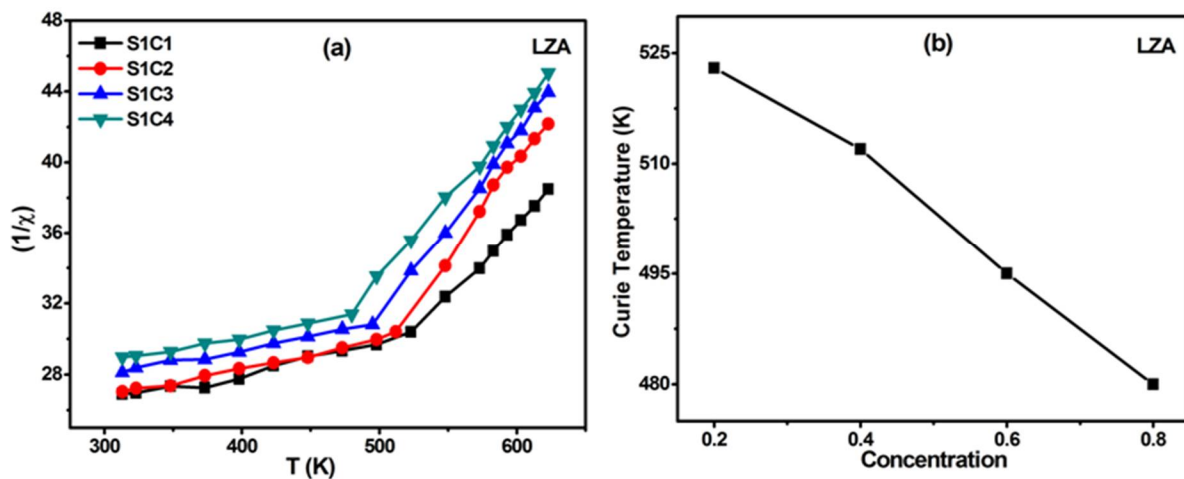


Fig. 3: (a) The variation of inverse of magnetic susceptibility ( $1/\chi$ ) versus temperature (b) The compositional variation of Curie temperature ( $T_C$ ) of series LZA spinel ferrite

## International Journal for Research in Applied Science & Engineering Technology (IJRASET)

**TABLE II**

CURIE TEMPERATURE and CURIE MOLAR CONSTANT of all SAMPLES of SERIES LZA at ROOM TEMPERATURE

Sample Code	Conc. y	T <sub>C</sub> (K)	C <sub>M</sub> (Obs.)	C <sub>M</sub> (Calc.)
S1C1	0.2	523	17.20	18.01
S1C2	0.4	512	16.84	17.51
S1C3	0.6	495	16.07	17.01
S1C4	0.8	480	15.29	16.51

The Curie temperature (T<sub>C</sub>) of all the sample of the series LZA spinel ferrite decreases gradually with the increase in Al<sup>3+</sup> substituent as shown in the fig. 3(b). This is attributed to replacement of Fe<sup>3+</sup> ions at the octahedral site in place of non-magnetic Al<sup>3+</sup> ions which results in decrease in B-sublattice magnetization. Consequently, the A-B exchange interaction between tetrahedral and octahedral sites would decrease and leading to decrease in the value of Curie temperature (T<sub>C</sub>) [20]. The observed and calculated values of Curie molar constants (C<sub>M</sub>) of series LZA spinel ferrite are listed in the table II. The theoretical values of Curie molar (C<sub>M</sub>) are calculated using “spin only” values. The observed values of Curie molar constants (C<sub>M</sub>) are slightly less than the theoretically calculated “spin only” values may attribute to slight non-collinear spin alignment or some amount of Fe<sup>3+</sup> is converted into Fe<sup>2+</sup> during synthesis.

#### IV. CONCLUSIONS

The saturation magnetization decreases due to substitution of non-magnetic Al<sup>3+</sup> ions. The low coercivity value indicates the soft magnetic nature of the material. The coercivity has inverse relationship with the grain size. The squareness ration (SQR) value is less than 0.5. It implies that the sample is produces of single magnetic domains which can be useful for microwave device applications. The value of Curie temperature (T<sub>C</sub>) decreases with increase in Al<sup>3+</sup> concentration. The observed values of Curie molar constants (C<sub>M</sub>) are slightly less than the theoretically calculated values may attribute to slight non-collinear spin alignment or some amount of Fe<sup>3+</sup> is converted into Fe<sup>2+</sup> during synthesis.

#### V. ACKNOWLEDGMENT

The Authors are very thankful to Sophisticated Analytical Instruments Facility (SAIF), STIC, IIT-Madras, Chennai for providing the VSM facility.

#### REFERENCES

- [1] M. Srivastava, S. Layek, J. Singh, A. Das, H. C. Verma, A. K. Ojha, N. H. Kim, J. H. Lee, “Synthesis, magnetic and Mössbauer spectroscopic studies of Cr doped lithium ferrite nanoparticles”, *J. Alloy. Comp.*, Vol. 591, pp: 174-180, 2014.
- [2] M. M. Hessian, “Synthesis and characterization of lithium ferrite by oxalate precursor route” *J. Magn. Magn. Mater.*, Vol. 320 (21), pp: 2800-2807, 2008.
- [3] Z. Yue, J. Zhou, X. Wang, Z. Gui, L. Li, “Preparation and studies of electrical properties of cobalt substituted Li-Zn ferrites by sol gel auto combustion method”, *J. Euro. Cera. Soci.*, Vol. 23 (1), pp: 189-193, 2003.
- [4] S.A. Jadhav, “Magnetic properties of Zn-substituted Li-Cu ferrites”, *J. Magn. Magn. Mater.*, Vol. 224, pp: 167-172, 2001.
- [5] P. R. Arjunwadkar, R. R. Patil, “Characterization of Al<sup>3+</sup> substituted lithium ferrite prepared by chemical method”, *J. Alloy. Comp.*, Vol. 611, pp: 273–277, 2014.
- [6] P. P. Hankare, R. P. Patil, U. B. Sankpal, S. D. Jadhav, P. D. Lokhande, K. M. Jadhav, R. Sasikala, “Investigation of structural and magnetic properties of nanocrystalline manganese substituted lithium ferrites”, *J. Solid State Chem.*, Vol. 182, p: 3217–3221, 2009.
- [7] B. D. Cullity, *Elements of X-ray diffraction*, Addison-Wesley Publ. Boston 1959.
- [8] L. Neel, “Magnetic properties of ferrites: ferrimagnetism and antiferromagnetism”, *Ann. Phys.*, Vol. 3, pp: 137-98, 1948.
- [9] L. Radhapiyari, S. A. Phanjoubam, H. N. K. Sharma, C. Prakash, “Electrical and magnetic studies of spinel system Li<sub>0.5+x</sub>Cr<sub>x</sub>Sb<sub>1-2x</sub>Fe<sub>2.5-x-2x</sub>O<sub>4</sub>”, *J. Phys. D: Appl. Phys.*, Vol. 32 (17), pp: 2151-2154, 1999.
- [10] M. A. Arillo, G. Cuello, M. L. Lopez, C. Pico, M. L. Veiga, “Crystal and magnetic structure of the system Li<sub>0.5+0.5x</sub>Fe<sub>2.5-1.5x</sub>Ti<sub>x</sub>O<sub>4</sub> (x= 0.16, 0.44, and 0.72) *Chem. Eur. J. Vol. 10* (21), pp: 5473-5480, 2004.
- [11] S. Verma, J. Karande, A. Patidar, P. A. Joy, “Lo-temperature synthesis of nanocrystalline powders of lithium ferrite by an autocombustion method using citric acid and glycine”, *Mater. Lett.*, Vol. 59 (21), pp: 2630-2633, 2005.
- [12] S. Verma, P. A. Joy, “Magnetic properties of superparamagnetic lithium ferrite nanoparticles”, *J. Appl. Phys. Vol. 98* (12), pp: 124312-124312-09, 2005.
- [13] S. M. Hoque, M. S. Ullah, F. A. Khan, M. A. Hakim, D. K. Saha, “Structural and magnetic properties of Li-Cu mixed spinel ferrite”, *Physica B: Condensed Matter*, Vol. 406 (9), pp: 1799-1804, 2011.

## International Journal for Research in Applied Science & Engineering Technology (IJRASET)

- [14] V. Verma, S. P. Gairola, V. Pandey, R. K. Kotanala, H. Su, "Permeability of Nb and Ta doped lithium ferrite in high frequency range", *Sol. Stat. Commun.*, Vol. 148 (3), pp: 117-121, 2008.
- [15] Mansour Al-Haj, "Microstructure characterization and magnetic behavior of  $\text{NiAl}_x\text{Fe}_{2-x}\text{O}_4$  and  $\text{Ni}_{1-y}\text{Mn}_y\text{Al}_{0.2}\text{Fe}_{1.8}\text{O}_4$  ferrites", *J. Magn. Magn. Mater.*, Vol. 311, pp: 517-522, 2007.
- [16] M. H. R. Khan, A. K. M. Akther Hossain, "Reentrant spin glass behavior and large initial permeability of  $\text{Co}_{0.5-x}\text{Mn}_x\text{Zn}_{0.5}\text{Fe}_2\text{O}_4$ ", *J. Magn. Magn. Mater.*, Vol. 324 (4), pp: 550-558, 2012.
- [17] Z. L. Wang, Y. Liu, Z. Zhang, *Handbook of Nanophase and Nanostructured Materials (Vol.III: Materials systems and Applications I)*, Kluwer Academic / Plenum Publishers, USA, 2003.
- [18] E. C. Stoner, E. P. Wohlfarth, "A mechanism of magnetic hysteresis in heterogeneous alloys", *Phil. Trans. Roy. Soc. London – A, Mathematical and physical sciences*, Vol. 240 (826), pp: 599-642, 1948.
- [19] R. V. Mangalaraja, S. Ananthakumar, P. Manohar, F. D. Gnanam, "Magnetic, electrical and dielectric behaviour of  $\text{Ni}_{0.8}\text{Zn}_{0.2}\text{Fe}_2\text{O}_4$  prepared through flash combustion technique", *J. Magn. Magn. Mater.*, Vol. 253 (1), pp: 56-64, 2002.
- [20] A. M. Sankpal, S. S. Suryavanshi, S. V. Kakatkar, G. G. Tengshe, R. S. Patil, N. D. Chaudhari, S. R. Sawant, "Magnetization studies on aluminium and chromium substituted Ni-Zn ferrites", *J. Magn. Magn. Mater.*, Vol. 186 (3), pp: 349-356, 1998.



10.22214/IJRASET



45.98



IMPACT FACTOR:  
7.129



IMPACT FACTOR:  
7.429



# INTERNATIONAL JOURNAL FOR RESEARCH

IN APPLIED SCIENCE & ENGINEERING TECHNOLOGY

Call : 08813907089  (24\*7 Support on Whatsapp)